COMPARISON OF *EL NIÑO*-SOUTHERN OSCILLATION MEASUREMENT PARAMETERS THROUGH ITS INFLUENCES ON TREE GROWTH RINGS

Daniela Oliveira Silva Muraja, Cecília Lemes Leite, Alan Prestes, Virginia Klausner.

Universidade do Vale do Paraíba/Instituto de Pesquisa e Desenvolvimento, Avenida Shishima Hifumi, 2911, Urbanova - 12244-000 - São José dos Campos-SP, Brazil, fys.dani@gmail.com, leitelemescecilia@gmail.com, aprestes@gmail.com, viklausner@gmail.com.

Resumo

This work analyzed the relationship between two El Niño-Southern Oscillation (ENSO) parameters, the Southern Oscillation Index (SOI) and the sea surface temperature in the NIÑO 3.4 region (NIÑO 3.4), with a ring width index (RWI) obtained from trees of *Araucaria angustifolia* species in Canela City (Southern Brazil). The chronology quality was calculated by series mean intercorrelation (rbt), expressed population signal (EPS), and signal-to-noise ratio (SNR). The findings show that ENSO does influence the climate in the Canela city region since both parameters gave very similar non-linear responses in the cross-wavelet coherence (WTC) analysis.
Palavras-chave: Dendrocronologia. Dendroclimatologia. EL NIÑO 3.4. SOI. ENSO.
Área do Conhecimento: Ciências Exatas e da Terra - Geociências.

Introdução

The study of global climate is crucial due to climate change's impact on nature and, consequently, human life (RENÉ; PATRICIO, 2007, WANG, 2019). "Climate" nowadays refers to ocean-atmosphere interaction controlling a continent's climate (WANG, 2019). Recent research focuses on understanding ocean-atmosphere variability to explain climate changes. However, limited instrument data (less than 100 years) with gaps exists, often due to equipment issues (RENÉ; PATRICIO, 2007). Many regions lack climate stations for measurements, including Brazil with problematic data in existing stations (GARREAUD, 1999), (RENÉ; PATRICIO, 2007).

The *El Niño*-Southern Oscillation - ENSO (Figure 1) impacts South American precipitation, leading to excessive wetness in southern Brazil and dry conditions in northern Brazil during its negative phase (*El Niño*) and the opposite conditions during the positive phase (*La Niña*) (RENÉ; PATRICIO, 2007). ENSO involves equatorial Pacific Sea Surface Temperature (SST) shifts and pressure changes between Tahiti and Darwin, Australia (BJERKNES, 1966, TRENBERTH,1997). This phenomenon combines *El Niño* events and the Southern Oscillation, influencing global climate with approximately 4 to 7-year periodicity (OLIVEIRA, 2001). During ENSO events, excess rainfall may cause floods, while droughts and heat waves may happen due to excessive drought (REBOITA *et al.,* 2012).

Figure 1 - Global effects of El Niño (left) and La Niña (right).

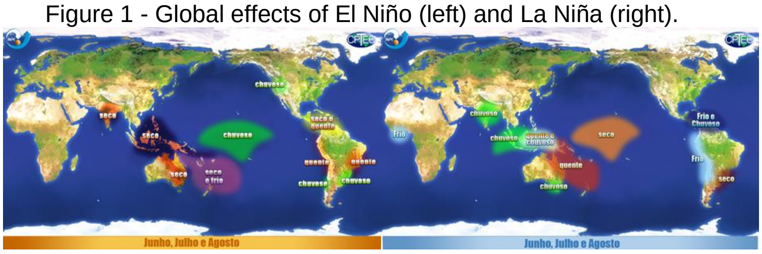

Source: INPE/CPTEC, 2016.

Dendrochronology combines tree ring analysis with climate data to infer past environmental conditions (SPEER, 1971). This method identifies climatic factors like temperature, precipitation, and events, aiding in modeling historical climate and contributing to global understanding, when direct climate records are unavailable. Tree rings play a significant role in Dendroclimatology, which studies climate-tree ring connections for paleoclimatic reconstructions, offering a unique opportunity to analyze climatic parameters, ocean-atmosphere events, and solar cycles, aiding in climate change understanding (SPEER, 1971, RAMSTEIN, 2021).Tree rings are used to reconstruct past climates, date

DOI: https://dx.doi.org/10.18066/inic0930.23

events, and assess human impacts on the environment. Understanding tree growth rings is widely used to identify and study the ENSO (PRESTES *et al.*, 2018, MURAJA *et al.,* 2023).

This work aims to obtain the response-growth of trees to the two parameters commonly used to measure the ENSO, and thus, compare these responses. Understanding the ENSO events and how it is measured is essential to understand the phenomenon since *El Niño* and *La Niña* events can cause droughts, floods, and other extreme weather events in various regions of the world, including the Southern region of Brazil.

Methodology

Araucaria angustifolia (Figure 2 left) is chosen for dendroclimatological analysis due to its wood's morphological and anatomical characteristics (Figure 2 right), ideal for dendrochronology (SANTAROSA *et al.,* 2007). This species is found in subtropical/temperate regions, facilitating climate variability study, and its longevity allows the construction of 100+ year chronologies. In Brazil, *Araucaria angustifolia* is widely studied, analyzing tree growth-climate responses and past climate reconstruction (CATTANEO *et al.,* 2013, MARTINKOSKI *et al.,* 2015, LORENSI, 2016, PRESTES *et al.,* 2018, SILVA *et al.,* 2021).

Figure 2 - *Araucaria angustifolia* species (left) and tree rings of an *Araucaria angustifolia* core (right). The Crown is the first growth year of the tree, earlywood is the wood formed at the beginning of a new ring and latewood is the wood formed at the end of the ring development, together they compound a tree ring.

Source: The Authors - Laboratório de Registros Naturais (LRN/UNIVAP).

Samples of *Araucaria angustifolia* were collected in 2005 via the non-destructive method (similar to a biopsy). Each tree yielded about 4 samples. Rings were made visible through transverse sanding (grits 300 to 50) and marked with a microscope for measurement. The samples were scanned at 1200 dpi using an EPSON Scanner, creating .jpg files. that were opened with the CooRecorder software, used to measure the rings. For crossdating and quality control, CDendro software ensured precise measurements and detected missing/false rings. Both software are available on the CYBIS website (https://www.cybis.se/forfun/dendro/).

The Regional Curve Standardization (RCS) is used as the detrending (filtering) methodology, applying a 67% spline to obtain a smooth curve, in order to maximize weather signals and minimize signals from any other influences. Tree-ring series are adjusted by division or subtraction based on age, resulting in an index. After filtering, time series are realigned to original years (HELAMA *et al.,* 2004, BUNN, 2018, HELAMA *et al.,* 2017, SILVA *et al.,* 2021).

To guarantee a final chronology with high quality the **Mean Series Intercorrelation** (r_{bt}) was computed, which is the mean of all the correlations between different pairs of samples, given by Equation 1.

$$r_{bt} = \frac{1}{N_{bt}}(r_{tot}N_{tot} - r_{wt}N_{wt}) \qquad \textbf{Equation 1}$$

considering r_{tot} as the mean of all correlations among different samples (within and between different trees), N_{tot} is the total number of samples, N_{wt} is the number of trees (COOK *et al.,* 1990), and r_{wt} is the within-tree signal obtained by averaging the coefficients between samples from the same tree. And N_{bt} is calculated by $N_{bt} = N_{tot} - N_{wt}$.

The **Expressed Population Signal (EPS)** was also calculated. It measures the proportion of variance of a population in a chronology that can be described by a finite subsample, telling how good the chronology is representing an infinite population (WIGLEY *et al.,* 1984, COOK *et al.*, 1990), (BRIFFA,

DOI: https://dx.doi.org/10.18066/inic0930.23

1900), in other words, guarantees that not one or a few samples are leading the chronology values (SILVA *et al.*,2021). EPS can be calculated by Equation 2.

$$EPS(t) = \frac{t * r_{bt}}{t * r_{bt} + (1 - r_{bt})} \qquad \textbf{Equation 2}$$

where t is the number of tree series.

And finally the **Signal-to-Noise Ratio (SNR)**, which gives the strength of the common signal in the trees and can be used instead of the EPS value (COOK *et al.*,1990). According to Wigley *et al.* (1984), it is defined by Equation 3.

$$SNR = \frac{N * r}{(1 - r)} \qquad \textbf{Equation 3}$$

considering N the number of trees and r the average correlation between the trees. The SNR tells how many times stronger the signals of the series are compared to the noise.

The Ring Width Index (RWI) can also be made by using the biweight robust mean. This is one way to help with noise reduction (outliers or extreme values) (MOSTELLER; TUKEY, 1977), since it automatically discounts the influence of noise values, reducing the variance caused by it (COOK *et al.*,1990). Equation 4 is used to obtain the chronology using biweight robust mean.

$$It = \sum_{j=1}^{m} w_t I_t \qquad \textbf{Equation 46}$$

and w_t is calculated by

$$w_t = \left[1 - \left[\frac{It - It*}{cS_t*}\right]^2\right]^2 \qquad \textbf{Equation 5}$$

for $\left[\frac{It - It*}{cS_t*}\right]^2 < 1$. Considering c as a constant defined by Mosteller and Tukey (1977), as 6 or 9. And finally, the $S_t *$ is the standard deviation of the frequency distribution obtained by the Equation 6 (COOK *et al.*,1990).

$$cS_t *= median(It - It *) \qquad \textbf{Equation 6}$$

The tree ring time series and the final chronology (ring width index - RWI) are shown in Figure 3.

Figure 3 - (a) Tree-ring time series. (b) Ring Width Index (RWI) is in black and the sample depth is in red.

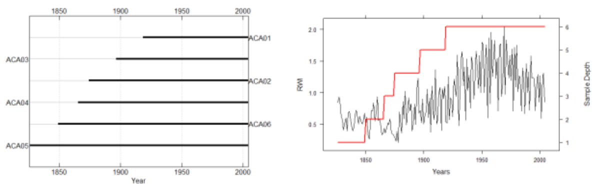

Source: The Authors.

The Southern Oscillation Index (SOI) is used to represent the pressure difference between Tahiti and Darwin calculated by (ROPELWSKI; HALPERT, 1987), it's accessible on the Climatic Research Unit website (https://crudata.uea.ac.uk/cru/data//soi/). Spanning 1866 to 2022, it's analyzed on an annual scale (Figure 4 left). SOI helps study ENSO events where >0 values indicate *La Niña*, and <0 signifies *El Niño (http://enos.cptec.inpe.br/*). To assess Equatorial Pacific's impact on precipitation and RWI, NIÑO 3.4 region (Figure 4 middle), located at 5°N - 5°S; 120°W - 170°W was chosen due to high *El Niño* variability (https://iridl.ldeo.columbia.edu/maproom/ENSO/Diagnostics.html). Figure 4 (right) shows *NIÑO* regions, with "NIÑO 3.4" amid "NIÑO 4" and "NIÑO 3". Monthly data from NCEP Database (https://www.cpc.ncep.noaa.gov/data/indices/) calculated as annual (Figure 4 top-right) for 1950 to 2023.

Figure 4 - Southern Oscillation Index time series and the NIÑO 3.4 region.

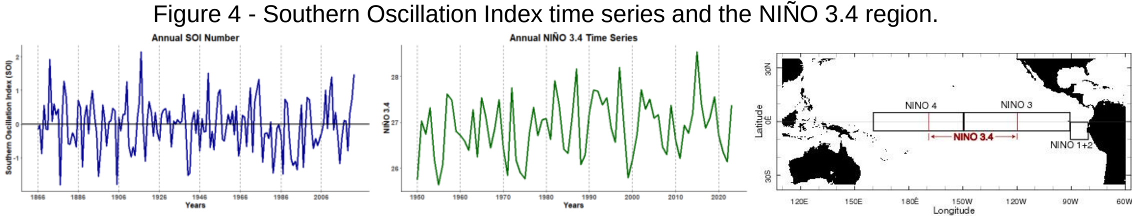

Source: The Authors.

DOI: https://dx.doi.org/10.18066/inic0930.23

The wavelet transform analyzes time series by decomposing them down into time-frequency space, revealing periodic patterns in both frequency and time. Here, the Continuous Wavelet Transform (CWT) is used on RWI, SOI, and NIÑO 3.4 time series to extract periodic signals. Wavelet transform is widely applied in dendrochronology, notably in *El Niño*-Southern Oscillation (ENSO) studies (GRINSTED *et al.,* 2004, RIGOZO *et al.,* 2012, PRESTES *et al.,* 2018, SILVA *et al.,* 2021, MURAJA *et al.,* 2023).

The time series x_n CWT is obtained by convolving x_n with a scaled "mother wavelet" function ψ by Equation 7. Edge effects due to finite time series are addressed with a Cone of Influence (COI), defined individually for each "mother wavelet." Morlet's COI, here employed, is $\sqrt{2}s$. Period scales align with each series' COI or its end (TORRENCE; COMPO, 1998).

$$W_n(s) = \sum_{n'=0}^{N-1} x_{n'}\psi * \left[\frac{(n'-n)\delta t}{s}\right] \quad \textbf{Equation 7}$$

To assess the non-linear relationship between the RWI and ocean-atmosphere and solar parameters, we employed cross-wavelet coherence (WTC). WTC gauges phase relationship between non-stationary time series in the time-frequency domain, extending classical coherence analysis used for non-stationary signals like climatic or geophysical series. Following (TORRENCE; COMPO, 1998), wavelet coherence for time series x_t and y_t is defined as Equation 8.

$$R_{xy} = \frac{\sum_{i=0}^{N-1} W_x^*(a,b,i)\cdot W_y(a,b,i)}{\left[\sum_{i=0}^{N-1} \left|W_x(a,b,i)\right|^2 \cdot \sum_{i=0}^{N-1} \left|W_y(a,b,i)\right|^2\right]^2}$$

Equation 8

All the analysis in this work was calculated through the RStudio scrips developed by Muraja, D.O. S., and can be accessed in the GitHub project DendrochronologySteps (https://github.com/MurajaDOS/DendrochronologySteps).

Results

Table 1 shows the rbt, EPS, and SNR values calculated. The rbt was calculated for the tree-ring time series, and EPS and SNR were calculated for the RWI.

Table 1 - Calculated statistics for the tree-ring time series (rbt), and for the RWI (EPS and SNR) to evaluate the quality of the final chronology (RWI).

rbt	EPS	SNR
0.474	0.844	5.399

Source: The Authors.

Figure 5 shows the Continuous Wavelet Transform (CWT) obtained for Canela RWI, SOI time series, and the NIÑO 3.4 time series. This transformation is the first step to analyzing possible patterns and performing the Cross-Wavelet Coherence (WTC) displayed in Figure 6.

Figure 5 - Continuous Wavelet Transform (CWT) for Canela RWI, SOI, and NIÑO 3.4. The CWT is the bottom graphic and the time series is the top graphic. The color bar shows the power of the CWT.

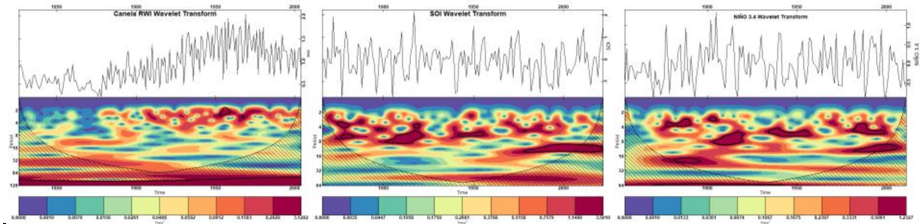

Source: The Authors.

DOI: https://dx.doi.org/10.18066/inic0930.23

Figure 6 - Cross-Wavelet Coherence (WTC) are the two top graphics showing Canela WTC (bottom), Canela RWI series (middle), SOI time series (top-left graphic - top), and NIÑO 3.4 time series (top-right graphic - top). The color bar shows the power of the WTC. The two bottom graphics are the SOI WTC and NIÑO 3.4 WTC averaged power, respectively.

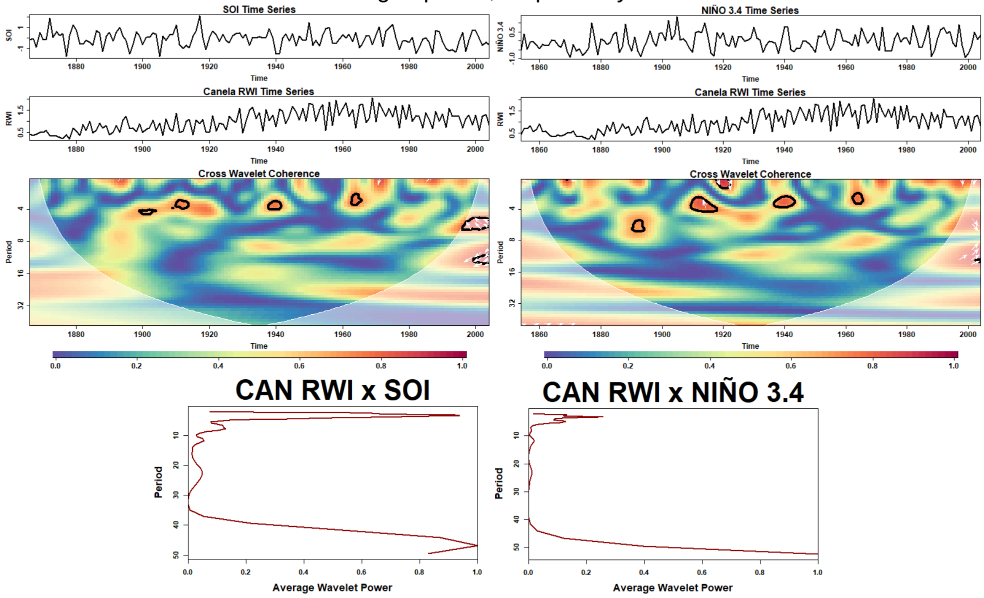

Source: The Authors.

Discussion

The rbt value calculated for the tree-ring series confirms that the analyzed trees are sharing the same influence in their growth signal. The EPS value suggests that all the trees collected in Canela are responding to the same limiting factor, and consequently, are well-dated. The SNR obtained value indicates that there is a consistent signal and not much noise in the final chronology.

The Canela RWI CWT (Figure 5 left) displays two significant periods, approximately 2-4 years, centered around 1950 and 1920, revealing short-term cyclic variations. The SOI data (Figure 5 middle) shows significance at about 2-8 years from 1885-1975, suggesting short-term cyclic variations reflecting El Niño-Southern Oscillation (ENSO) interannual variations. Another significant period is 8-16 years from 1975-2010, implying ENSO's decadal variations. NIÑO 3.4 CWT (Figure 5 right) aligns with SOI results, also indicating various significant periods. Notably, 16-32 years from 1875-1900 is significant, mirroring SOI's ENSO-related components that vary across interannual (2-8 years) to decadal (8-16 years) and longer scales. These similarities are expected as both the SOI and NIÑO 3.4 are essential components of the El Niño-Southern Oscillation (ENSO) phenomenon, which exhibits variability at various time scales, ranging from interannual (2-8 years) to decadal (8-16 years) and longer.

The analysis of the WTC between Canela RWI and SOI (Figure 6 left) provided small significant regions approximately in the period of 4, around the years 1900, 1915, 1940, and 1965. The WTC results for NIÑO 3.4 and Canela RWI (Figure 6 right) show almost the same years as the WTC for the SOI. The differences are that the periods extend from 2 to 8 periods, and were obtained periodicities around 1890, 1910 (anti-phase), and 1920 (in-phase), which may indicate just a lagged response of the tree's growth to the ENSO events. The averaged power shows similar powers for the <10 period and for the >40 period, however, the power is stronger when using SOI to analyze the relationship with the Canela RWI.

Conclusion

This study examined the link between a ring width index (RWI) derived from Araucaria angustifolia trees in Canela City, Southern Brazil, and two El Niño-Southern Oscillation (ENSO) parameters: the Southern Oscillation Index (SOI) and sea surface temperature in the NIÑO 3.4 region (NIÑO 3.4). The outcomes affirm ENSO's influence on the Canela region's climate, as both parameters show similar non-linear responses in cross-wavelet coherence (WTC) analysis. Moreover, we found that the SOI WTC has a strong power when compared with the NIÑO 3.4 WTC. This suggests that the SOI might be more readily detected within tree-growth signals.

DOI: https://dx.doi.org/10.18066/inic0930.23

References

BUNN, A. G. A dendrochronology program library in R (dplR). **Dendrochronologia.,** v. 26, n. 2. Disponível em: https://doi.org/10.1016/j.dendro.2008.01.002.

BJERKNES, J. A possible response of the atmospheric Hadley circulation to equatorial anomalies of ocean temperature. **Tellus.,** v. 18, n.4, 1966. Disponível em: https://doi.org/10.1111/j.2153-3490.1966.tb00303.x.

CATTANEO, F. A.; ANDREO, C. R.; RODRIGUES, R. R.; AMARAL, M.; ANAND, M.; STOFFEL, M. Climate signals in tree-ring widths of Araucaria angustifolia in an altitudinal gradient in southern Brazil. **Trees.**, v. 27, n. 5, 2013. Disponível em: 10.1007/s00468-013-0884-y.

COOK, E.; BRIFFA, K.; SHIYATOV, S.; MAZEPA, V. Tree-ring standardization and growth-trend estimation. **Methods of Dendrochronology: Applications in the Environmental Sciences.,** 1990.

GARREAUD, R. D.; BATTISTI, D. S. Interannual (ENSO) and interdecadal (ENSO-like) variability in the Southern Hemisphere tropospheric circulation. **Journal of Climate.,** v.12, 1999.

GRINSTED, A.; MOORE J. C.; JEVREJEVA , S. Application of the cross wavelet transform and wavelet coherence to geophysical time series. **Nonlinear Processes in Geophysics.** v. 11, n. ⅚. Disponível em: 10.5194/npg-11-561-2004.

HELAMA, S.; LINDHOLM, M.; TIMONEN, M.; ERONEN, M. Detection of climate signal in dendrochronological data analysis: a comparison of tree-ring standardization methods. **Theoretical and Applied Climatology.,** v 79, 2004.

HELAMA, S.; THOMAS, S. M. M.; KEITH, R. B. Regional curve standardization: State of the art. **The Holocene.,** v. 29, n. 1, 2017.

LORENSI, C. **Resposta dos anéis de crescimento de Araucaria angustifolia (Bertol.) O. Kuntze da região sul do Brasil aos forçantes geofísicos e climáticos**. 2016. Dissertação- Universidade do Vale do Paraíba – UNIVAP, Instituto de Pesquisa e Desenvolvimento Programa de Pós-Graduação em Física e Astronomia.

MARTINKOSKI, L.; HIGA, A. R.; BRANDALISE, R.; STIVAL, S. M. L.; ANAND, M. Climatic influences on the radial growth of Araucaria angustifolia in the Brazilian South Atlantic Forest. **iForest - Biogeosciences and Forestry,** v. 9, 2015.

MOSTELLER, F.; TUKEY, J. W. **Data Analysis and Regression: A Second Course in Statistics.** Reading, MA: Addison-Wesley Pub Co., 1977.

MURAJA, D. O. S.; KLAUSNER, V.; PRESTES, A.; SILVA, I. R. Ocean–atmosphere interaction identified in tree-ring time series from southern Brazil using cross-wavelet analysis. **Theoretical & Applied Climatology,** 2023.

RAMSTEIN, G.; LANDAIS, A.; BOUTTES, N; SEPULCHRE, P.; GOVIN, A. **Paleoclimatology**. Springer, 2021.

REBOITA, M. S.; KRUSCHE, N.; AMBRIZZI, T.; ROCHA, R. P. Entendendo o Tempo e o Clima na América do Sul. **Terra E Didática.,** v. 8, n. 1, 2012.

RENE, D. G.; PATRICIO, A. **The Physical Geography of South America.** New York: OXFORD UNIVERSITY PRESS, 2007.

RIGOZO, N.; LISI, C.; FILHO, M.; PESTES, A.; NODERMANN, D.; PEREIRA S. E. M.; ECHER, E.; EVANGELISTA, H.; RIGOZO, V. Solar-Terrestrial Signal Record in Tree Ring Width Time Series from Brazil. **Pure and Applied Geophysics.,** v. 169, 2012. Disponível em: 10.1007/s00024-012-0480-x.

ROPELEWSKI, C. F.; JONES, P. D. An Extension of the Tahiti–Darwin Southern Oscillation Index. **Monthly Weather Review.,** v. 115, n.9, 1987. Disponível: https://doi.org/10.1175/1520-0493(1987)115<2161:AEOTTS>2.0.CO;2.

SANTAROSA, E.; OLIVEIRA, J. M.; ROIG, F. A.; PILLAR, V. D.; Crescimento sazonal em araucaria angustifolia: Evidências anatômicas. **Revista Brasileira de Biociências,** v. 5, 2007.

SILVA, D. O.; PRESTES, A.; KLAUSNER, V.; SOUZA T. G. G. Climate Influence in Dendrochronological Series of Araucaria angustifolia from Campos do Jordão, Brazil. **Atmosphere.** v. 12, n. 8, 2021. Disponível: 10.3390/atmos12080957.

SPEER, J. H. **Fundalmentals of Tree-Ring Research.** Library of Congress Cataloging-in-Publication Data, 1971.

OLIVEIRA, S. G. El Niño e Você – o fenômeno Climático. **Transtec Editorial.** 2001.

PRESTES, A.; KLAUSNER, V.; GONZALES, A. O.; SILVA, I. R. Resposta do Crescimento da Araucaria à Variabilidade Solar e Climática na Região de Passo Fundo - RS. In: "V Simpósio Brasileiro de Geofísica Espacial e Aeronomia - SBGEA, 2018.

TRENBERTH, K. E. The Definition of El Niño. **Bulletin of the American Meteorological Society.,** v. 78, n.12, 1997.

TORRENCE, C.; COMPO G. P. A Practical Guide to Wavelet Analysis.**Bulletin of the American Meteorological Society.,** v. 79, n. 1, 1998.

WANG, C. Interações de três oceanos e variabilidade climática: uma revisão e perspectiva. **Clim Dyn.,** n. 52**,** 2019.

WIGLEY, T. M. L.; BRIFFA, K. R,.; JONES, P. D. On the Average Value of Correlated Time Series, with Applications in Dendroclimatology and Hydrometeorology. **Journal of Applied Meteorology and Climatology.,** v. 23, n. 2, 1984. Disponível em: https://doi.org/10.1175/1520.

Acknowledgment

This work was carried out with the support of Coordenação de Aperfeiçoamento de Pessoal de Nível Superior (CAPES) – Doctorate scholarship PROSUC - 88887.714652/2022-00 and the Conselho Nacional de Desenvolvimento Científico e Tecnológico - Scientific Initiation Scholarship - Projeto Universal - CNPq/MCTI/FNDCT N°18/2021.

DOI: https://dx.doi.org/10.18066/inic0930.23